

Coherent Nuclear-Spin Interactions of Adsorbed ^{131}Xe Gas with Surfaces

Z. Wu and W. Happer

Department of Physics, Princeton University, Princeton, New Jersey 08544

and

J. M. Daniels

Department of Physics, University of Toronto, Toronto, Canada M5S 1A7

(Received 8 June 1987)

By using highly asymmetric glass cells, we have increased the wall-induced quadrupole splitting of the nuclear-spin sublevels of noble-gas atoms by some 2 orders of magnitude over previously reported values. We have used these large surface interactions to make quantitative studies of the electric field gradients experienced by the nuclei of ^{131}Xe atoms adsorbed on glass walls.

PACS numbers: 76.60.Es, 33.30.+a, 68.45.Da, 82.65.My

Simpson and co-workers^{1,2} first discovered that the spin- $\frac{3}{2}$ nuclei of ^{201}Hg relax at a rate which depends on the asymmetry of the quartz cell used to contain the Hg vapor and on the orientation of the cell with respect to the external magnetic field. Similar effects were observed by Volk and co-workers^{3,4} for spin-polarized ^{83}Kr and ^{131}Xe nuclei. These unusual phenomena were due to coherent wall interaction; i.e., the slowly relaxing nuclei of these gaseous systems behave as though they were situated in an equivalent static electric-field gradient equal to the ensemble-averaged value of the field gradient experienced by the nucleus of the gas atom at every adsorption site on the cell wall.

In this Letter we report the first quantitative studies of coherent surface interactions. We have investigated

^{131}Xe atoms which have been polarized by spin-exchange collisions with optically pumped Rb atoms in glass cells. The experimental arrangement is shown in Fig. 1. The cylindrical Pyrex glass cells have a diameter d and height h . Typically d is about 1.3 cm and h varies between 0.3 and 1 cm. The cells contain a few milligrams of Rb metal with natural isotopic abundance, and about 5 Torr (at 25 °C) of ^{131}Xe gas which has been isotopically enriched to an assay of 70% ^{131}Xe , which has a nuclear spin $K = \frac{3}{2}$. The cells usually contain 50 Torr of N_2 gas. The cells are heated in an oven to temperatures in the range 70 °C to 100 °C by flowing hot air.

The Xe nuclei are polarized by spin-exchange pumping for a few minutes with Rb atoms which are maintained nearly fully spin polarized by optical pumping

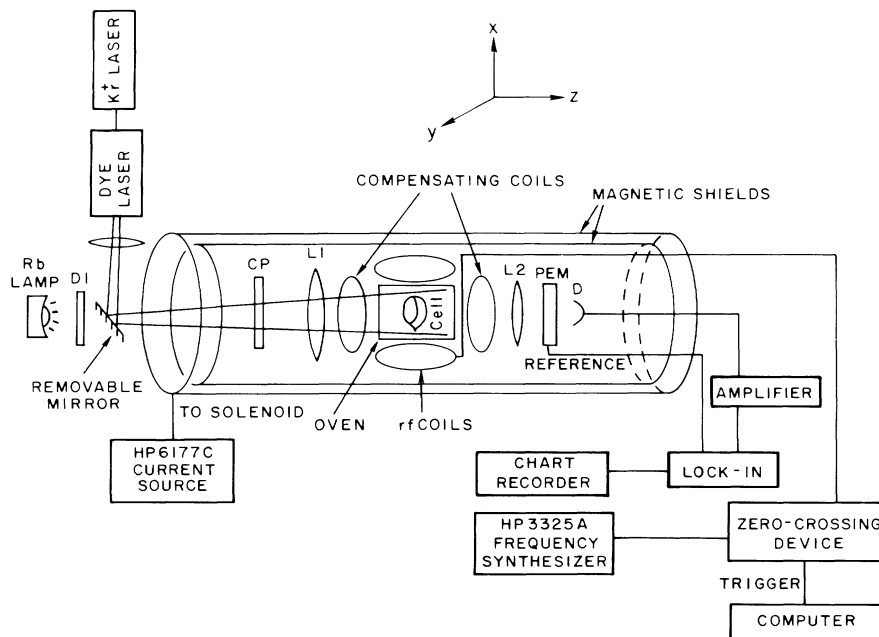


FIG. 1. The main parts of the apparatus, as described in the text.

with about 400 mW of circularly polarized 7948-Å light from a cw dye laser, pumped by a krypton-ion laser. Once the nuclei have been polarized, the laser light is blocked and the spin polarization is probed by the passing of unpolarized 7948-Å D_1 light from a Rb resonance lamp through a cell. This light then passes through a photoelastic modulator before it is collected by a silicon photodiode. The photoelastic modulator is used to detect the small amount of circular polarization of the probe light, which is proportional to the longitudinal nuclear spin $\langle K_z \rangle$ of the ^{131}Xe atoms. More details about the physics of the detection process can be found in the work of Zeng *et al.*⁵

The wall interactions are observed with the help of transient nuclear magnetic resonance.⁶ A static magnetic field B_0 (in the direction of the z axis) of about 0.1 G is produced by a solenoid, surrounded with two concentric Mumetal shields which reduce the field fluctuations to less than 1 mG. An optically pumped Cs magnetometer, not shown in Fig. 1, is located within 3 cm of the sample cell and is used to sense the total magnetic field. Any fluctuations in the field are canceled by feedback of current into the compensating coils of Fig. 1. This active stabilization holds the longitudinal field at the cell constant to within $2 \mu\text{G}$. At the beginning of the probe phase of the experiment we apply a magnetic field of the form $2B_1 \sin \omega t$ along the x axis. The oscillating field can be thought of as the vector sum of two fields of magnitude B_1 , rotating uniformly at the angular velocities ω and $-\omega$ around z axis. We ordinarily choose $\omega \approx \omega_0$, where ω_0 is the Larmor frequency of the nuclei in the static magnetic field B_0 . Consider a coordinate system rotating at the frequency ω around the z axis. In this system the nuclei will precess at the frequency

$$\Omega = [(\omega_0 - \omega)^2 + \omega_1^2]^{1/2}. \quad (1)$$

Here ω_1 , the Rabi frequency, is the Larmor frequency of the nuclei in a field B_1 . The precession axis ζ is tilted by an angle $\psi = \cos^{-1}[(\omega_0 - \omega)/\Omega]$ from the z axis. The cell appears to rotate backwards about the z axis at a frequency ω , but since the rotational symmetry axis of the cell coincides with the z axis, the cell is effectively at rest in the rotating coordinate system and any slight structural asymmetries—for example, the asymmetry due to the sealoff—are averaged out.

A typical transient signal from ^{131}Xe is shown in Fig. 2(a). The oscillating magnetic field was turned on at time $t=0$, and the oscillation frequency ω was chosen to be equal to the magnetic resonance frequency ω_0 so that the tilt angle was $\psi=90^\circ$. This signal was obtained from a Pyrex glass cell, 1.28 cm in diameter and 0.68 cm in height, which contained natural Rb metal, 5 Torr of ^{131}Xe , and 49.4 Torr of N_2 . The Fourier transform of the transient signal, shown in Fig. 2(b), contains a “carrier” frequency at 476.3 mHz and “sidebands” with the frequencies 443.2 and 506.5 mHz. As indicated in the inset, these frequencies can be identified with the Bohr

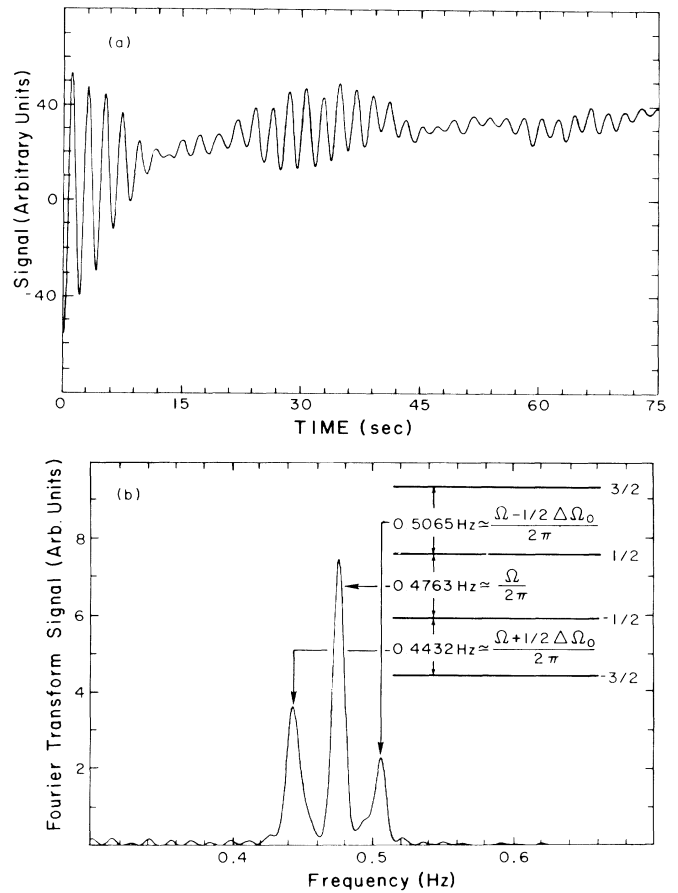


FIG. 2. (a) The precession signal of ^{131}Xe for the cell described in the text. The signal is proportional to $\langle K_z \rangle$, the longitudinal nuclear spin of ^{131}Xe in the laboratory coordinate system. (b) The Fourier spectrum of the signal in (a), and the energies of the nuclear-spin sublevels in the rotating coordinate system. The three resonances are peaked at the Bohr frequencies of the three $\Delta m = 1$ transitions. In ordering the energy sublevels, we have assumed that $\Delta\Omega_0 < 0$.

frequencies of the $\Delta m = 1$ transitions between quantum states of the ^{131}Xe nucleus in the rotating coordinate system.

The phenomenon illustrated in Fig. 2 can be understood with the following simple argument. From kinetic theory we know that each Xe atom makes $vS/4V$ collisions/sec with the cell wall, where S is the surface area, V is the volume of the cell, and v is the mean thermal velocity of the Xe gas atoms. The fraction of the time in which a Xe atom experiences an appreciable wall interaction is $vS\tau_s/4V$, where τ_s is the mean sticking time of a Xe atom on the wall. The effective Hamiltonian H_{eff} is given by the product of this fraction and the wall interaction Hamiltonian, averaged over the sticking time τ and over the entire inner surface of the container,

$$H_{\text{eff}} = \left\langle \frac{vS\tau}{4V} \int_S \frac{dS'}{S} \int_0^\tau \frac{dt}{\tau} H_w \right\rangle. \quad (2)$$

The brackets in (2) denote an ensemble average over the microscopic interaction history of an adsorbed atom. For ^{131}Xe the wall interaction is completely dominated by the coupling of the nuclear quadrupole-moment tensor Q_{ij} to the electric field gradients $\partial^2 V/\partial x_i \partial x_j$ which arise when the atom is near the wall, and so we can write $H_w = \frac{1}{6} Q_{ij} \partial^2 V/\partial x_i \partial x_j$. The symmetry of the situation requires that any residual part of H_w which does not average to zero must be given by

$$\left\langle \int_0^\tau H_w dt \right\rangle = \frac{\hbar \langle \theta \rangle}{2K-1} \left[(\mathbf{K} \cdot \mathbf{n})^2 - \frac{K(K+1)}{3} \right], \quad (3)$$

where \mathbf{n} is a unit vector normal to the surface element dS and directed from the vapor into the glass wall. The angle $\langle \theta \rangle$, the mean twist of the nuclear polarization produced by the quadrupole interaction during a collision, is defined by

$$\langle \theta \rangle = \frac{3eQ}{4K\hbar} \left\langle \int_0^\tau dt \left[\frac{\partial^2 V}{\partial n^2} - \frac{1}{3} \nabla^2 V \right] \right\rangle, \quad (4)$$

with Q the conventional quadrupole moment of the nucleus and e the elementary charge.

Consider a cylindrical sample cell of diameter d and height h with its symmetry axis along the z axis. Substituting (3) into (2) and carrying out the surface integral, we find that

$$H_{\text{eff}} = \hbar \Delta \Omega_0 \left[\frac{3K_z^2 - K(K+1)}{3(2K-1)} \right], \quad (5)$$

where the quadrupole splitting frequency is

$$\Delta \Omega_0 = \frac{1}{2} v \langle \theta \rangle (1/h - 1/d). \quad (6)$$

The total Hamiltonian in the rotating coordinate system is then

$$H = \hbar \Omega K_\zeta + H_{\text{eff}}. \quad (7)$$

Under the conditions of our experiments ($|\Omega| \approx 3 \text{ rad sec}^{-1}$, $|H_{\text{eff}}/\hbar| \approx 0.2 \text{ rad sec}^{-1}$), we may regard H_{eff} as a small perturbation in (7) and write the energy eigenvalues of H as $E_m = m \hbar \Omega + E_m^{(1)} + E_m^{(2)} + \dots$, where the n th-order energy shift $E_m^{(n)}$ of a sublevel with azimuthal quantum number m along the ζ axis can be calculated from perturbation theory. The first-order shift is readily found to be

$$E_m^{(1)} = \hbar \Delta \Omega_0 P_2(\cos \psi) \frac{3m^2 - K(K+1)}{3(2K-1)}, \quad (8)$$

where $P_2(x) = \frac{3}{2}x^2 - \frac{1}{2}$ is the second-order Legendre polynomial. Thus, we expect that the nuclear polarization in the rotating coordinate system will contain the frequencies of the three $\Delta m = 1$ transitions sketched in Fig. 2(b), i.e., Ω and $\Omega \pm \Delta \Omega_0 P_2(\cos \psi)$. The longitudinal polarization $\langle K_z \rangle$ in the laboratory system will also contain these frequencies, and these are in fact the frequencies shown in Fig. 2(b). The quadrupole splitting

frequency $|\Delta \Omega_0|$ can be determined from the sideband splittings and from the known tilt angle ψ . One can readily vary the tilt angle by changing the frequency ω or magnitude ω_1 of the oscillating field, and we have verified experimentally that the sideband displacements are proportional to $P_2(\cos \psi)$ as predicted by (8). We note that the beats of Fig. 2 can be eliminated by adjustment of the oscillating field parameters to make $\psi = 54.7^\circ$ where $P_2(\cos \psi) = 0$. We have also verified experimentally that the slightly unequal spacings of the sidebands of Fig. 2(b) are well described by the higher-order contributions to E_m .

We have measured $|\Delta \Omega_0|$ for many cells and the results are shown in Fig. 3. As predicted by (6) we find that $|\Delta \Omega_0|$ is directly proportional to the asymmetry parameter $(h^{-1} - d^{-1})$ of the cells. Using the mean thermal velocity $v = 2.39 \times 10^4 \text{ cm sec}^{-1}$ for a Xe atom at a temperature of 82°C , we obtain the characteristic twist angle $|\langle \theta \rangle| = (38 \pm 4) \times 10^{-6} \text{ rad}$.

We find that Pyrex glass surfaces reach an equilibrium or "cured" state after exposure to Rb-metal vapor for several days at temperatures of about 85°C . During the curing process the beat period decreases from initial values which are often too long to observe to the final values plotted in Fig. 3. Once a cell has been cured, no significant changes are noticed in the beat period or in the damping rate if the Rb droplets are redistributed within the cell by distillation with a hand torch.

We have measured the dependence of the relaxation rate and the beat period of the transient signal on the pressure of the N_2 gas, and we found that these quantities were almost independent of pressure between 20 and 240 Torr, as one would expect, since in this range of pressures the diffusion time to the cell wall ($\approx 10^{-2} \text{ sec}$) is short compared with the observed precession time ($\approx 1 \text{ sec}$).

The damping of the signal in Fig. 2(a) is almost en-

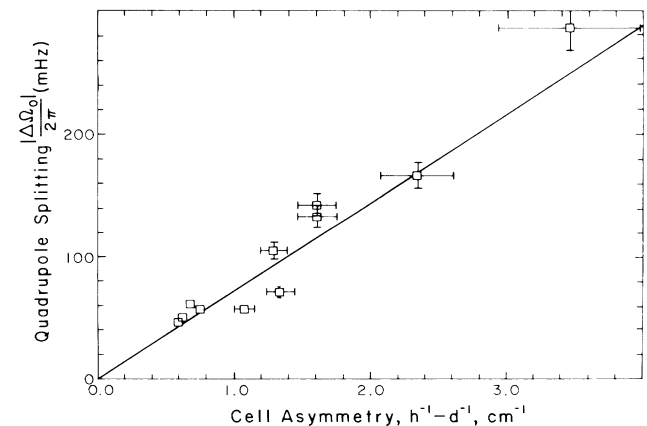


FIG. 3. The measured dependence of the characteristic beat frequencies, $|\Delta \Omega_0/2\pi|$, on the cell asymmetry parameter $(h^{-1} - d^{-1})$. The slope of this line is $v|\langle \theta \rangle|/4\pi$.

tirely due to wall interactions since the gas-phase interactions⁵ of ¹³¹Xe lead to a relaxation time of about 500 sec. The quadrupole interactions on the wall appear to be nearly isotropic, and so we may use the theory of quadrupolar wall relaxation developed by Cohen-Tannoudji⁷ to write for the orientation damping rate

$$\gamma_1 = (c/5)(1/h + 2/d)\langle\theta^2\rangle, \quad (9)$$

where

$$\langle\theta^2\rangle = \frac{\tau_c \tau_s^2}{\tau_c + \tau_s} \left[\frac{eQ}{2\hbar} \left(\frac{\partial^2 V}{\partial z'^2} - \frac{1}{3} \nabla^2 V \right) \right]^2. \quad (10)$$

Here τ_s is the mean dwell time of a Xe atom on the wall, τ_c is the correlation time of the fluctuating field gradient, and $\partial^2 V/\partial z'^2 - \frac{1}{3} \nabla^2 V$ is the field gradient along an axis of cylindrical symmetry, which was assumed to have a random direction in Ref. 7. Substituting the observed 25-sec damping time and the dimensions of the cell of Fig. 2 into (9), we find the mean-square twist angle $\langle\theta^2\rangle = (2.8 \pm 0.3) \times 10^{-6} \text{ rad}^2$. Nearly the same values of $\langle\theta^2\rangle$ are found for all of the cells of Fig. 3.

A small, measured temperature dependence of $|\Delta\Omega_0|$ can be adequately described by the assumption that $\Delta\Omega_0$ is proportional to an Arrhenius factor, $\exp(-E_a/kT)$, with the activation energy $E_a = -0.03 \pm 0.01 \text{ eV}$. The cured glass surfaces described here probably differ substantially from bare Pyrex, for which the adsorption energy has been measured⁸ to be about 0.3 eV. Furthermore, weakly adsorbed Xe atoms may make a disproportionately large contribution to the coherent wall interaction and its activation energy.

Adsorbed Xe gas has been used as an important probe of surfaces,⁹ and the coherent surface interactions de-

scribed here could probably be used to study new properties of surfaces, including catalytic surfaces. It would also be possible to use beat frequencies like those of Fig. 2 to measure the quadrupole moments of radioactive noble-gas nuclei in experiments analogous to those described by Kitano *et al.*¹⁰

We are very grateful to Masao Kitano for his valuable help during the course of this experiment. The work was supported by the U.S. Air Force Office of Scientific Research under Grant No. 81-0104-C.

¹D. S. Bayley, I. A. Greenwood, and J. H. Simpson, unpublished.

²J. H. Simpson, *Bull. Am. Phys. Soc.* **23**, 394 (1978).

³C. H. Volk, J. G. Mark, and B. Grover, *Phys. Rev. A* **20**, 2381 (1979).

⁴T. M. Kwon, J. G. Mark, and C. H. Volk, *Phys. Rev. A* **24**, 1894 (1981).

⁵X. Zeng, Z. Wu, T. Call, E. Miron, D. Schreiber, and W. Happer, *Phys. Rev. A* **31**, 260 (1985).

⁶C. P. Slichter, *Principles of Magnetic Resonance* (Springer-Verlag, Berlin, 1978).

⁷C. Cohen-Tannoudji, *J. Phys. (Paris)* **24**, 653 (1963); We have made the following corrections to formulas in this reference: The right-hand side of (2) should be multiplied by $-\frac{1}{2}$. The right-hand side of (5b) should be multiplied by $(4\pi)^{-1}$. The right-hand side of (12) should be multiplied by $(16\pi\hbar^2)^{-1}$.

⁸R. Ahrens-Botzong, P. Hess, and K. Schäfer, *Ber. Bunsenges. Phys. Chem.* **77**, 1157 (1973).

⁹R. J. Birgenau and P. M. Horn, *Science* **232**, 329 (1986).

¹⁰M. Kitano, M. Bourzutschky, F. P. Calaprice, J. Clayhold, W. Happer, and M. Musol, *Phys. Rev. C* **34**, 1974 (1986).